JOURNAL OF SPACECRAFT AND ROCKETS
Vol. 31, No. 6, November–December 1994

Aerodynamic Design of Pegasus™: Concept to Flight with Computational Fluid Dynamics

Michael R. Mendenhall,* Daniel J. Lesieutre,† Steven C. Caruso,‡ Marnix F. E. Dillenius,§ and Gary D. Kuhn¶
Nielsen Engineering & Research, Inc., Mountain View, California 94043

Pegasus™, a three-stage, air-launched, winged space booster, was developed to provide fast and efficient commercial launch services for small satellites. The aerodynamic design and analysis of the vehicle were conducted without wind-tunnel and subscale model testing, using only computational aerodynamic and fluid-dynamic methods. All levels of codes, ranging in complexity from empirical database methods to three-dimensional Navier-Stokes codes, were used in the design. This article describes the design and analysis requirements, the unique and conservative design philosophy, and the analysis methods considered for the various technical areas of interest and concern.

Nomenclature

AR	= aspect ratio
C_D	= drag coefficient
C_L	= lift coefficient
C_m	= pitching-moment coefficient
C_N	= normal-force coefficient
$\bar{c}$	= mean aerodynamic chord
g	= gravitational acceleration
h	= altitude
l	= reference length
M_∞	= Mach number
p	= local pressure
p_∞	= freestream pressure
q_∞	= dynamic pressure
S	= reference area
t	= time
x	= axial coordinate measured from the nose
y	= lateral coordinate
z	= vertical coordinate
α	= angle of attack, deg
β	= angle of sideslip, deg
δ	= horizontal tail deflection angle, deg
ϕ	= angle of roll, deg
λ	= taper ratio

Subscripts

cp	= center of pressure
m	= center of moments

Introduction

PEGASUS (Fig. 1) is an air-launched space booster designed to satisfy launch requirements for small payloads in a variety of missions. The objective of this privately financed development program is to provide reliable space launch services at a low cost on a near-term schedule. Under this joint venture between Orbital Sciences Corporation and Hercules Aerospace Company, the design approach is based on a conservative development using conventional techniques while exploiting state-of-the-art technology and experience. The aerodynamic design and analysis was based on proven, readily available computational codes, and no wind-tunnel tests were performed as part of the program.

The aerodynamic analysis and support considered a number of different technical areas such as trajectory requirements, aerodynamic loading distributions, stability and control, and aerodynamic heating.[1] The flight conditions included carriage and launch from the B-52 parent aircraft, transonic flight at high angles of attack, supersonic flight over the entire angle-of-attack range, and hypersonic flight to first-stage burnout. For this entire flight regime, it was necessary to select and validate appropriate prediction methods, estimate the level of accuracy achieved, and limit the flight envelope as necessary according to experience and engineering judgement.

The computational techniques used, from engineering methods (empirical, database, theoretical codes) to computational fluid dynamics (CFD) methods, and the results obtained from each level of prediction method are presented. Though specific codes will be described, it is not the purpose of this article to evaluate individual codes, but to evaluate the approach of using a number of different codes for detailed aerodynamic design of a new flight vehicle for which no test data exist. Portions of this article previously appeared as part of Ref. 1.

Background

Pegasus Mission

To gain the advantages of increased payload performance and operational flexibility, Pegasus is carried aloft beneath the wing of a B-52 bomber. The performance improvements over ground launch are a result of both the aircraft forward velocity and the initial launch altitude. Launch at 40,000 ft contributes to lower dynamic pressure, lower drag, and lower structural and thermal stresses. The reduced atmospheric pressure range encountered by the first stage permits optimization of the first-stage nozzle.

In level flight at Mach 0.8 and 40,000 ft, Pegasus is released from the carrier aircraft and allowed to free-fall for 5 s. After first-stage ignition, Pegasus begins a 2.5-g pullup maneuver using wing lift and thrust while accelerating through the transonic speed regime and maximum dynamic pressure. When first-stage burnout occurs after 82 s, the vehicle has reached Mach 8.7 at an altitude of over 200,000 feet. The first stage, which includes all the aerodynamic lifting surfaces, is separated from the second and third stages at this time. A typical baseline flight profile is illustrated in Fig. 2. The end of the aerodynamic analysis is at first-stage burnout.

Geometry

A sketch of the complete configuration is shown in Fig. 1. The blunt-nose body is cylindrical with a constant diameter of about 4 ft over the total body length of 50 ft. A fairing between the wing and the body and a slight flare near the tail to accommodate the nozzle of the first-stage rocket engine are the only modifications to

Received Oct. 19, 1990; Presented as Paper 91-0190 at the AIAA 29th Aerospace Sciences Meeting, Reno, NV, Jan. 7–10, 1991; revision received June 10, 1992; accepted for publication March 19, 1993.

*Vice President. Associate Fellow AIAA.
†Research Engineer. Member AIAA.
‡Research Scientist. Member AIAA.
§President. Associate Fellow AIAA.
¶Senior Research Scientist. Associate Fellow AIAA.

the cylindrical shape. The graphite composite wing, a clipped delta planform with a modified double wedge airfoil section, is mounted on top of the fuselage, slightly aft of midlength. The wing span of 22 ft is dictated by the available clearance from the B-52 aircraft and is the same as for the X-15 research aircraft. The position of the wing is critical to minimize the pitching-moment variation due to the large center-of-gravity travel during first-stage burn.

The tail section is composed of horizontal stabilizers with clipped delta planform and a vertical rudder. These all-movable surfaces are also double wedge sections made of graphite composite material. Other important details of the geometry that must be considered in the aerodynamic analysis are the interaction of the wing and tail surfaces and the contours and corners produced by the wing-body fairing.

Although significantly different from the X-15 geometry, there are a number of similarities between the configurations that are dictated by the B-52 carriage and launch requirements (Fig. 1b).

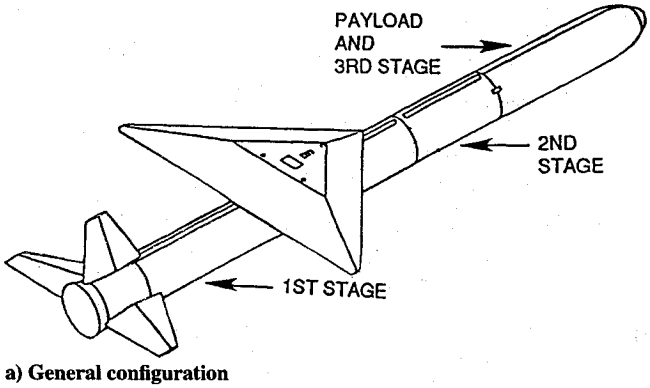

a) General configuration

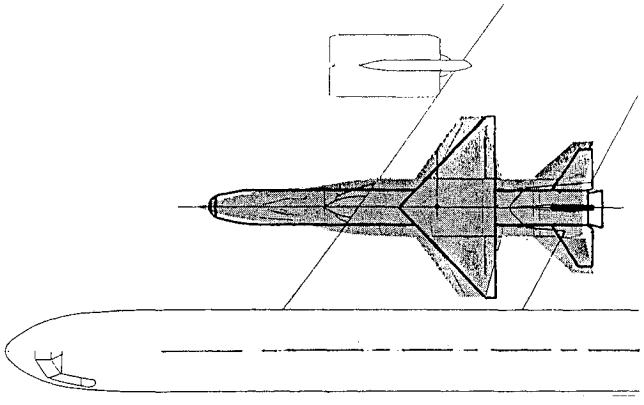

b) Comparison of Pegasus and X-15 carriage positions on B-52

Fig. 1 Pegasus.

Given these similarities, the aerodynamic characteristics of Pegasus can be compared with measured and predicted X-15 aerodynamics to check the computational results.

Aerodynamic Requirements

A typical baseline mission profile for Pegasus is shown in Fig. 2 to illustrate the aerodynamic requirements during the first 80 s of the mission. Briefly, launch from the B-52 occurs at $M_\infty = 0.8$ at a low angle of attack. The angle of attack immediately increases to nearly 20 deg as Pegasus accelerates through the transonic regime to supersonic speed. During this part of the mission, Pegasus is gaining altitude using both rocket thrust and wing lift. By $M_\infty = 3$, the angle of attack is down to 5 deg, and by $M_\infty = 6$ it is nearly 0. Different missions will dictate different angle-of-attack and Mach-number envelopes.

A typical flight envelope is illustrated by the solid curve in Fig. 3, and the names of various computer codes are shown to illustrate their range of applications. Before a decision about appropriate aerodynamic prediction methods can be made, the aerodynamic requirements for the various technical areas are needed. A minimum set of requirements is shown in Table 1. For trajectory simulations, the longitudinal and lateral aerodynamic characteristics must include effects of control-surface deflections, since trim calculations are required throughout the trajectory. Some of the other items in Table 1 are specific to Pegasus; for example, the wing-fairing shock interference is of interest because of a specific vehicle component, and the B-52 pylon carriage loads and separation trajectories are required because of the nature of the launch. The number of flow conditions shown for each requirement is a conservative estimate based on preliminary design considerations. In reality, items such as the longitudinal and lateral aerodynamic matrices were calculated each time the design changed; therefore, the 1400 flow conditions shown were calculated as many as four different times.

Aerodynamic Design Philosophy

Economics, accuracy, and schedule were under constant consideration during the computational aerodynamic analyses. In some cases, the number of calculations required dictated the codes and methods that could be used; for example, even if it were technically possible, the aerodynamic matrices could not be developed using CFD methods because of the cost and time involved. These aerodynamic characteristics were calculated using simpler, faster engineering methods. However, certain of the calculations involving flow separation and shock-wave interference are too complex for simple methods, and these results can only be obtained using modern CFD techniques involving solutions of the Navier-Stokes equations. In other cases, intermediate methods such as panel methods and solutions of the Euler equations provided the design details required.

Additional considerations in the aerodynamic design philosophy were code availability, ease of use, engineering capability, and confidence level. Obviously, codes that are difficult to acquire and use cannot be considered for a design study like Pegasus, because of the time constraints involved. Also, there is little time available for code

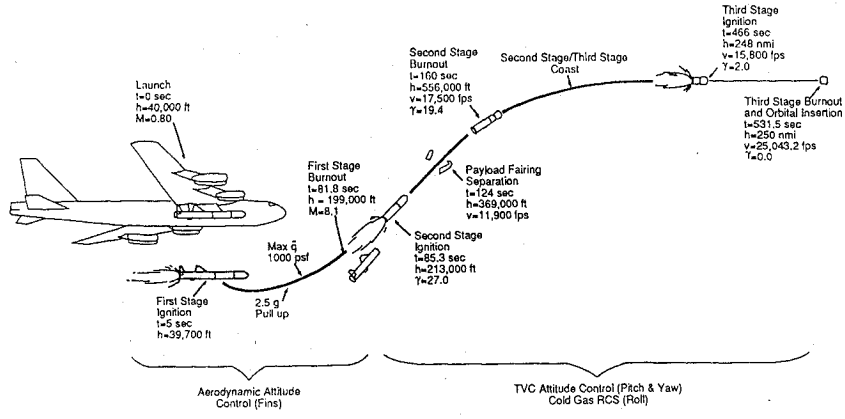

Fig. 2 Pegasus baseline mission profile.

Table 1 Predicted aerodynamic requirements

Trajectory simulations	Flow conditions
Longitudinal matrix $(M_{\infty},\alpha,\delta)$	504
Lateral matrix $(M_{\infty},\alpha,\beta,\delta_A,\delta_R)$	918
Wing and fin detail design loads	4
Nose distributed loads	1
Plume-induced separation	3
Wing-fairing shock interference	2
B-52 pylon carriage loads	3
Separation trajectory	4

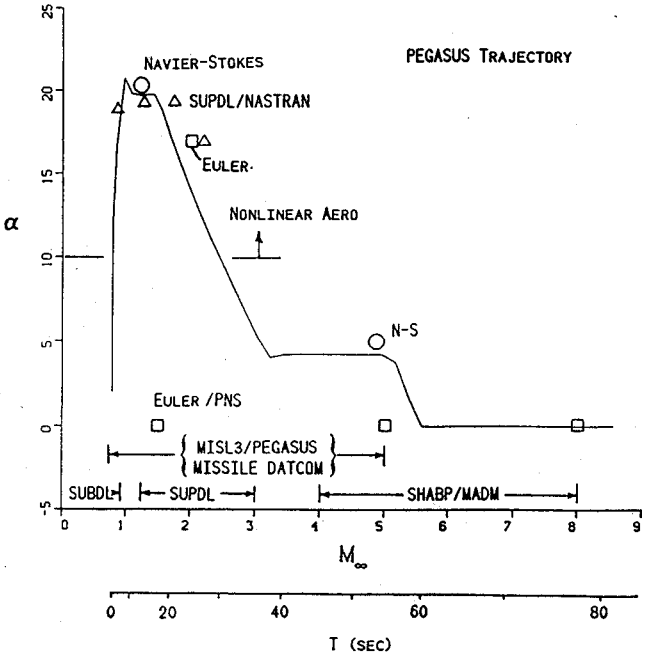

Fig. 3 Aerodynamic analyses flight envelope.

development and training; therefore, reliable codes familiar to the design group are a necessity. Finally, since no specific wind-tunnel data on Pegasus are available for guidance, there must be a high degree of confidence in the prediction methods so that a large amount of time is not spent validating the selected codes. The objective of the Pegasus effort was to use the highest-level code required for a specific task.

In this commercial design effort, time became an important factor since the goal was two years from design initiation to the first flight. The basic aerodynamic analysis had to be completed quickly in the conceptual design stage so that the design effort could move on toward final design. As geometric modifications were made, rapid aerodynamic evaluation was necessary so that performance characteristics were available in a timely manner for mission analysis.

After the preliminary aerodynamic design, there is generally more time available for aerodynamic support. For example, the calculation of aerodynamic heating and aerodynamic loads for structural design require the use of more complex methods, but the timing, though still important, is not as critical. Similarly, very detailed fluid-mechanic analysis of certain flow characteristics may require a significant effort using modern CFD methods, but the results of this study, though important for the final design, may be carried out over a longer period of time after the final aerodynamic design is fixed. The method-selection process for this design effort is described in greater detail in the next section.

Technical Discussion and Results

A number of different aerodynamic design and analysis codes were applied to Pegasus; the portions of the flight envelope considered by various codes are shown in Fig. 3. The different codes used are identified in Table 2, and descriptions of each code are presented in the following paragraphs. Since it is important to see the relationship between the specific aerodynamic task and the code or codes selected, sample results are presented and discussed at the same time the prediction methods are described.

Table 2 Prediction methods

Code	Developed by	Description
MISL3	NEAR (DOD/NASA)	Database/theory
DATCOM	McDAC (AF)	Database/theory
SUBDL	NEAR (Navy)	Panels/viscous effects
SUPDL	NEAR (NASA)	Panels/viscous effects
SHABP	McDAC (AF)	Shock exp/impact theory
MADM	McDAC (AF)	Shock exp/impact theory
SWINT	NSWC	Euler
UPS	NASA/AMES	Parabolized Navier-Stokes
ARC2D	NASA/AMES	Two-dimensional N-S
TURF	NASA/AMES	Axisymmetric N-S
F3D	NASA/AMES	Three-dimensional N-S
SUBSTR	NEAR (AF/Navy)	Subsonic store separation

Preliminary Design

Speed and accuracy are important considerations for the codes used for preliminary design purposes. A number of possible codes are available for this task, but not all codes are applicable to the configuration and flow conditions of interest for this investigation.[2] Since no experimental data on Pegasus were to be available, a conservative approach was taken for the analysis, and a number of different codes were selected for the preliminary aerodynamic design phase.

Two independent engineering codes for preliminary design and analysis, MISL3[3,4] and Missile DATCOM,[5,6] were used in parallel to predict the longitudinal and lateral aerodynamic characteristics of Pegasus over the first part of the flight envelope below Mach 5. Between Mach 4 and 8, the S/HABP[7] and MADM[8] codes were selected.

MISL3 is a semiempirical code that uses a combination of theoretical methods with nonlinear corrections for the body and an extensive experimental data base for wing-alone and fin-on-body loads. The data base inherently includes viscous and compressibility effects as well as fin-body gap effects. The code emphasizes high angles of attack and transonic speeds, important flow regimes for Pegasus. Mutual interference between control surfaces is also considered in the data base, another important feature for the anticipated flight profile. To provide some confidence in the applicability of this code, MISL3 has been validated by comparison of measured and predicted aerodynamic characteristics with a number of different configurations.[3,4,9,10] The range of application of the flow parameters in the MISL3 data base is

$$0.5 \le M_{\infty} \le 5.0, \qquad 0.25 \le \mathrm{AR} \le 4.0$$
$$-45.0 \le \alpha \le 45.0, \qquad 0.0 \le \lambda \le 1.0$$
$$0.0 \le \phi \le 90.0$$

Missile DATCOM is based on the body-buildup method and includes a number of empirical prediction methods for each component of the configuration. It was developed specifically for preliminary design applications, and it has also been validated by numerous comparisons with experimental data.[5,10,11] Even though MISL3 and Missile DATCOM use some similar approaches, they are independent codes with individual strengths and weaknesses. For example, Missile DATCOM predicts axial force or drag much better than MISL3, but MISL3 predicts vortex-induced forces and moments at high angles of attack better. The body loads in Missile DATCOM have proved to be more accurate than those from MISL3 for subsonic flow.

Both of these codes provide independent predictions of Pegasus aerodynamics. Throughout the preliminary aerodynamic analysis, both codes were run in parallel for all flow conditions and the results

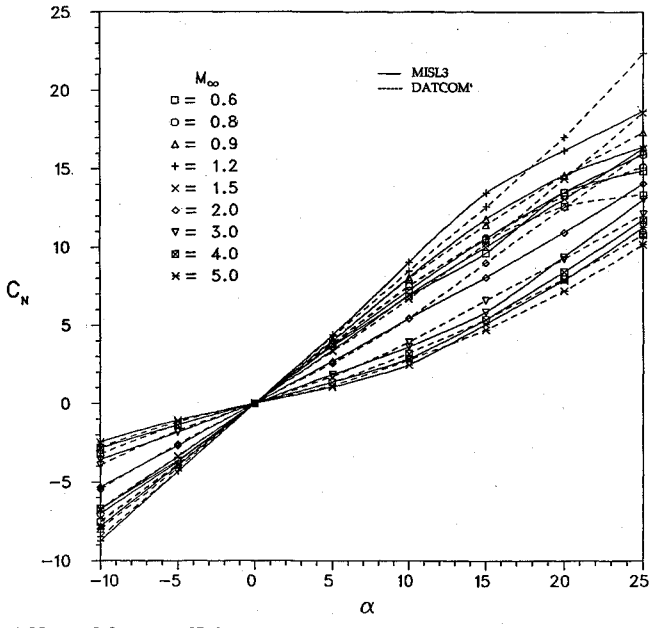

a) Normal-force coefficients

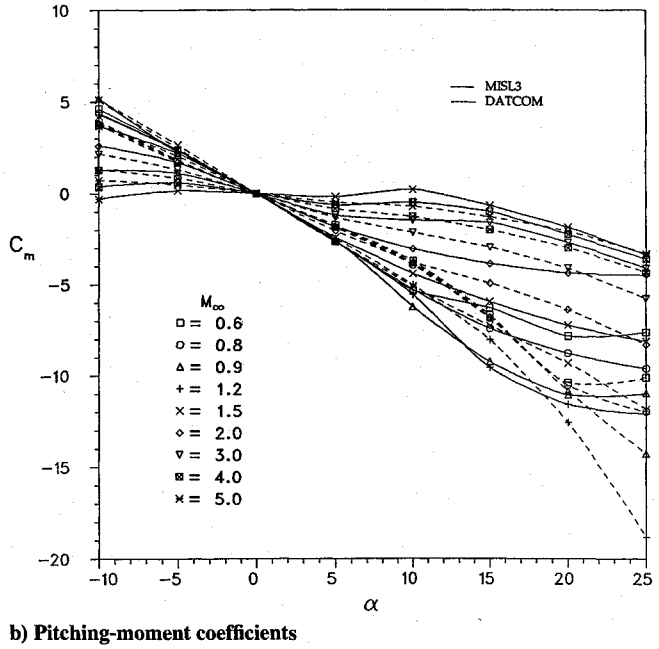

b) Pitching-moment coefficients

Fig. 4 Comparison of MISL3 and Missile DATCOM longitudinal aerodynamic characteristics.

were compared. Since some of the flight regime involves high angles of attack where vortex-induced nonlinearities can dominate the aerodynamic characteristics, there is likely to be some disagreement between the results from the two codes. When this occurs, higher-level codes can be used to predict a limited number of results to help resolve the differences.

Predicted static longitudinal aerodynamic characteristics of the complete Pegasus configuration with control surfaces undeflected are shown in Fig. 4 for a range of Mach numbers. Results from both MISL3 and Missile DATCOM are shown. Agreement is very good for the entire range of Mach numbers at moderate angles of attack, but there is some disagreement above $\alpha = 10$ deg, a good indication that predicted vortex effects are different between the two codes. The final aerodynamic characteristics are determined by a combination of the two results, giving consideration to the respective strengths of both codes. One application of these aerodynamic results is for trajectory simulations; therefore, the calculations were repeated for a range of horizontal tail deflection angles to complete the longitudinal aerodynamic matrix.

A matrix of Pegasus lateral aerodynamic characteristics was generated by varying the sideslip angle and the rudder deflection angle. Roll control information was generated by computing the effects of differential deflection of the horizontal tail surfaces.

Verification of the above approach for longitudinal aerodynamic characteristics was essential to build confidence in the calculation procedure. Experimental results are available[12] on a similar configuration at $M_\infty = 2$, and comparisons of measured and predicted lift, drag, and center of pressure are shown in Fig. 5 for a range of angles of attack up to the maximum angle permitted for the Pegasus mission. The comparisons are in very good agreement. Since the longitudinal center of pressure was not in as good agreement as the force coefficients, a sensitivity study was performed to illustrate the effect of moving the moment center an amount equal to 10% of the mean aerodynamic chord. It is apparent that this is approximately the magnitude of the error in the predicted center of pressure.

The two previous codes have an upper limit of Mach 5; therefore, another code was required for the higher Mach number ranges. Missile DATCOM has a hypersonic option, which was used at selected flow conditions; however, other codes may be more appropriate to this flow regime. S/HABP[7] and MADM[8] were applied to Pegasus for Mach numbers between 4 and 8. Note that there is also an overlap in the Mach region at which preliminary design codes were used to be certain of continuity of results. MADM is a major upgrade of the S/HABP code and includes additional capability to improve the pressure prediction at supersonic speeds. Both codes are panel codes that use impact methods to predict pressure distributions on arbitrary configurations. The disadvantages with these codes are the absence of wing-tail vortical interference effects and the requirement that the user select the appropriate force calculation procedure from the many options. However, it is possible to validate the codes with experimental or other predicted results. Since the angle of attack at the higher Mach numbers is typically very low, and it is expected that the aerodynamic characteristics are well-behaved, MADM was used for most of the calculations. The MADM results were compared with MISL3 and Missile DATCOM results between Mach 4 and 5 to verify consistency and accuracy.

Predicted lift and drag coefficients at $M_\infty = 8$ are shown in Fig. 6 for a range of angles of attack and tail deflection angles far beyond that expected during flight. An impact-panel representation of Pegasus is also shown in the figure. No data on a similar configuration in this Mach range are available for comparison purposes.

Engineering Methods

The next level of code available for aerodynamic calculations is a panel method. For Pegasus, the high angles of attack experienced at both subsonic and supersonic speeds add the requirement that vortex-induced effects be included. These vortex effects are those associated with vortex shedding from the body ahead of the wing. SUPDL,[13] an improved version of the NWCDM-NSTRN supersonic code, was immediately available for analysis over the Pegasus flight envelope up to Mach 3. A subsonic version, SUBDL,[14] was also available for use in the limited flight regime between launch and the onset of transonic flow.

SUPDL represents the components of the configuration with distributions of singularities derived from supersonic linear theory. The body is modeled with linearly varying supersonic line sources and doublets to account for volume and angle-of-attack effects, and the lifting surfaces and body interference regions are modeled with planar supersonic lifting panels. Nonlinear fin loads associated with leading-edge and side-edge separation at high angles of attack are included. Other important nonlinearities from forebody and afterbody separation vortices are included, as is the interference effect of the wing trailing vorticity on the tail fins. SUPDL also has the capability of predicting the aerodynamic characteristics of the configuration under constant pitch, yaw, and roll rates. This is particularly useful for obtaining damping derivatives to a first approximation.

The predicted distributions of aerodynamic loads from both SUBDL and SUPDL are easily converted for use in the structural analysis code NASTRAN. This information on the wing and tail fins at a number of different flow conditions was provided to the structural designers. Predicted loading distributions on the

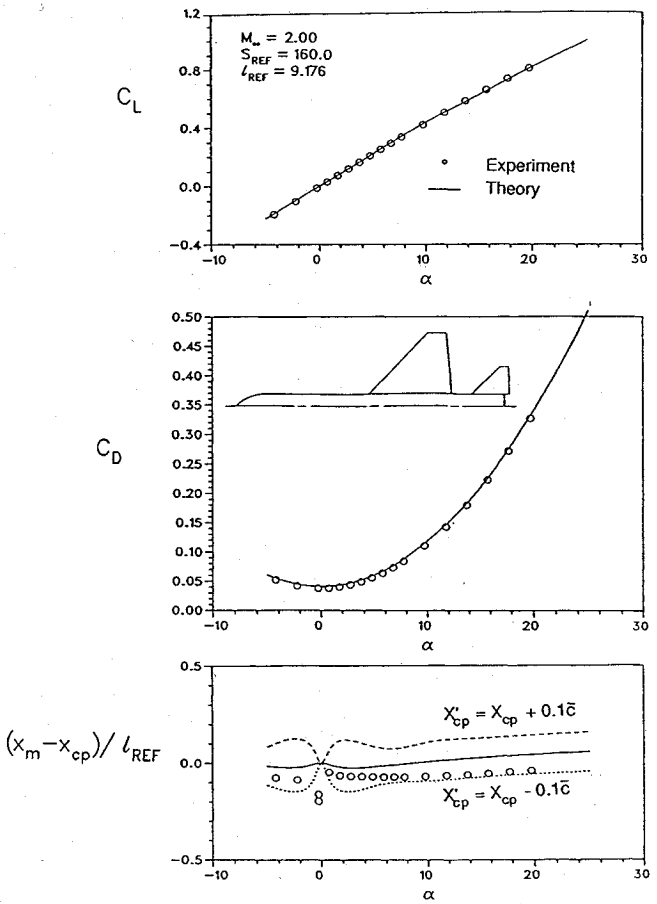

Fig. 5 Measured and predicted longitudinal aerodynamic characteristics of a wing-body-tail configuration.

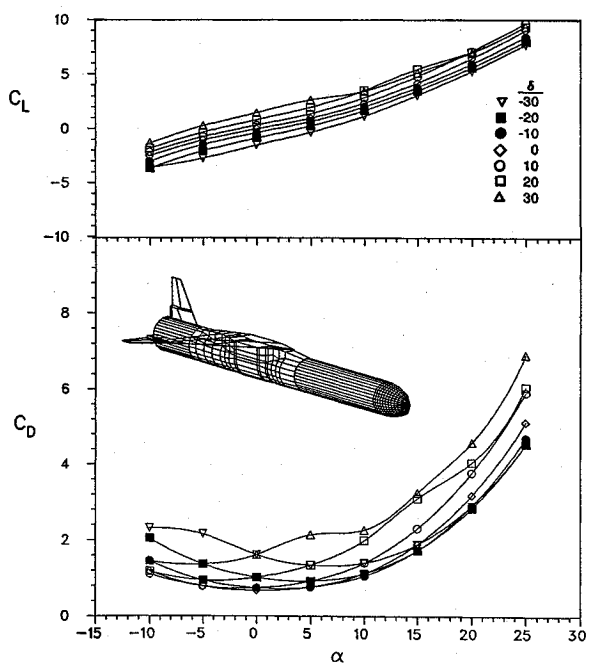

Fig. 6 Predicted aerodynamic characteristics at $M_\infty = 8$.

wing in subsonic and supersonic flow at a high angle of attack are shown in Fig. 7. The arrows represent the magnitude of the aerodynamic loading at specific wing locations considered in the aerodynamic analysis.

Carriage and Launch Methods

Areas that do not bear directly on the aerodynamic design of Pegasus are the carriage and launch characteristics. The carriage

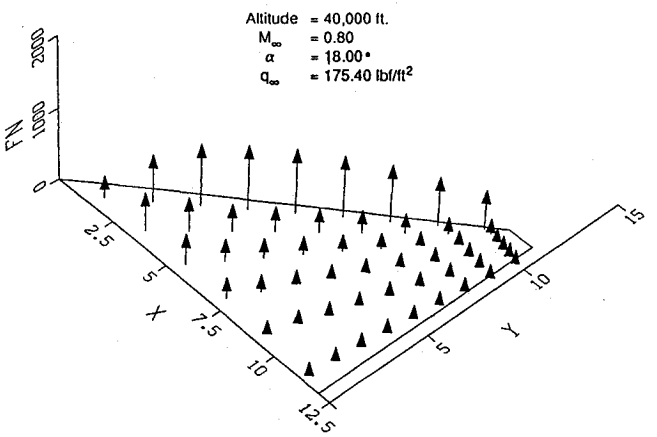

a) SUBDL code

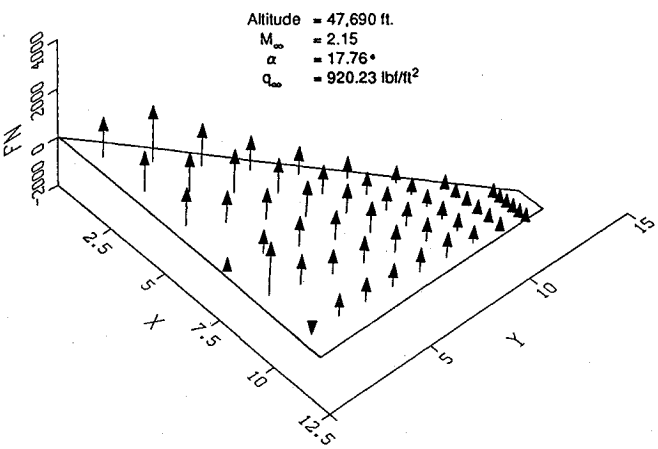

b) SUPDL code

Fig. 7 Predicted aerodynamic loading distribution on the Pegasus wing.

loads are critical to the design of the B-52 pylon adaptor as well as flight safety and mission viability. The launch characteristics are important not only for the safety of the launching aircraft but for the initial flight conditions of Pegasus. These characteristics can be measured experimentally, but the expense and delay in the design schedule were not practical for this commercial effort; therefore, an analytical approach was selected.

Carriage loads and launch characteristics require that Pegasus's aerodynamic loads be known in the flowfield of the launching aircraft, a B-52 for the initial analysis. Previous work in the prediction of store separation from various aircraft,[15] including the B-52,[16] provided the necessary capability. Previous validation of these methods[17] on a number of different store-separation problems was sufficient to give confidence in the predicted results.

Carriage loads were calculated using both the loads prediction method in the store-separation code, SUBSTR,[15] and the panel code SUBDL[14] integrated into SUBSTR. In each case Pegasus was placed in the predicted nonuniform flowfield associated with the B-52 at various flight conditions. Altitude, airspeed, and perturbations to the flight path caused by gusts were considered. Forces and moments on Pegasus were predicted, and the loads on the pylon attachment points were calculated and examined for possible problems.

Launch characteristics were calculated using SUBSTR[15] with its six-degree-of-freedom trajectory simulation capability. For this analysis, Pegasus is launched from the B-52 with all controls inactive and neutral for the first 5 s; therefore, the initial flight trajectory while in the influence of the B-52 determines the position and attitude of Pegasus at ignition. The first 3 s of a normal launch are shown in Fig. 8. Notice that Pegasus falls away from the B-52 with a slightly nose-down attitude and small roll angle away from the fuselage. The predicted Pegasus trajectory is in good agreement with measured and predicted X-15 trajectories;[18] however, the pitch

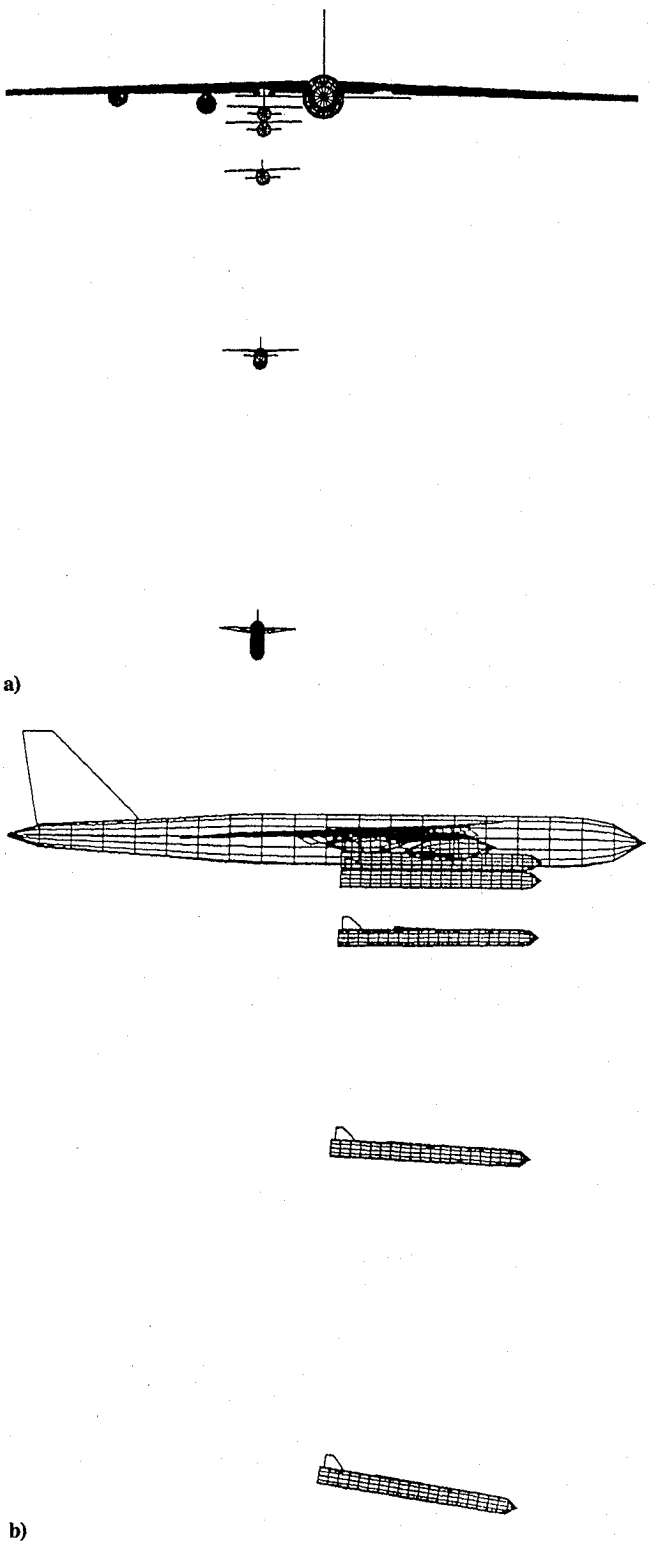

a)

b)

Fig. 8 Simulated Pegasus standard drop from the B-52, SUBSTR code, $M_\infty = 0.8, t = 0, 0.5, 1.0, 2.0,$ and 3.0 s.

and roll angles associated with Pegasus are much less than those experienced by the X-15.

Another feature of the analytical launch-prediction method is its ability to investigate nonstandard launch characteristics. Though not planned, Pegasus might be dropped with controls locked in various fully deflected positions corresponding to pitch, yaw, or roll control; it is essential to identify a priori any emergency launches that could endanger the B-52 aircraft. A number of extreme launch conditions were simulated with SUBSTR. In every case Pegasus cleared the B-52 and fell safely away from the aircraft.

Other Methods

Based on the results presented above, the missile designer may begin to believe that all aerodynamics problems can be solved with one code or another. Before that happens, it is time to return to reality and examine the calculation of static and dynamic stability derivatives, an important area in which large uncertainties exist in analytical methods.

The Missile DATCOM, MISL3, SUBDL, and SUPDL codes have the capability of calculating important stability derivatives, and, following established procedures, several independent methods were used to build the confidence level for the results. Static longitudinal and lateral derivatives are available from Missile DATCOM and MISL3 at specified flow conditions between Mach 0.6 and 5.0. The results from the MADM code were in good agreement with these results between Mach 4 and 5; therefore, MADM was used for predictions to Mach 8. The SUBDL and SUPDL codes were used to check the above results at selected flow conditions at moderate Mach numbers, and this higher-level calculation verified the simpler methods.

The prediction of dynamic stability derivatives has higher uncertainty, and there are few codes available for this task. A method[19] based on supersonic linear theory had proved successful for the X-15, and this approach was applied to Pegasus. As a check on this approach, the code SUPDL was applied to the Pegasus configuration, and the pitch, roll, and yaw damping results are in good agreement with the linear theory.[1]

Fortunately, the similarity between the X-15 and Pegasus provides a means to estimate the quality of the predicted stability derivatives. Experimental measurements of the stability characteristics of the X-15 are available,[20] and, in general, the static and dynamic derivatives predicted for Pegasus and measured on the X-15 are similar in nature over the entire flight range. Comparisons of Pegasus and X-15 longitudinal and lateral stability derivatives are presented in Ref. 1.

Computational Fluid Dynamics

As shown in Fig. 3 and Table 2, a number of CFD codes were used for detailed flow simulations. Calculations have been made with an Euler code, a parabolized Navier-Stokes code, two-dimensional and axisymmetric Navier-Stokes codes, and a three-dimensional Navier-Stokes code. Different applications of various CFD codes are described below to illustrate the use of these advanced techniques in practical configuration design and analysis.

Euler Solutions

SWINT[21] has been used for a number of different calculations during the Pegasus analysis. First, it was used to predict the dynamic-pressure defect on the lee side of the configuration at supersonic speeds to assess rudder effectiveness for lateral-stability analyses. This correction is included as part of the MISL3 code. Euler calculations were also used to predict detailed fuselage loads for the nose-fairing design.

Parabolized Navier-Stokes Solutions

In the early design phase of Pegasus, a potential for separation of the flow near the aft end of the fuselage, caused by the first-stage rocket plume, was identified. Since a separated-flow region would occur in the vicinity of the control fins (Fig. 1), a significant loss in fin effectiveness could occur if the fins were immersed in this flow. A rapid CFD analysis was proposed to determine the possibility of flow separation in this region. Considering the flight envelope shown in Fig. 3, most of the flight occurs near an angle of attack less than 5 deg; therefore, to further simplify the CFD analysis, the angle of attack was assumed zero, the wing and fins were neglected, and calculations were performed for the body only. These assumptions permit an axisymmetric analysis, which considerably reduces the required computational effort.

Flow-separation calculations were performed at three Mach numbers, 1.5, 5, and 8, corresponding to Mach numbers on the baseline mission profile. A zonal calculation approach using three different computer codes was used for the supersonic analysis. First, an Euler blunt-body code[22] was used to compute the axisymmetric flow over a sphere to approximate the flow in the vicinity of the

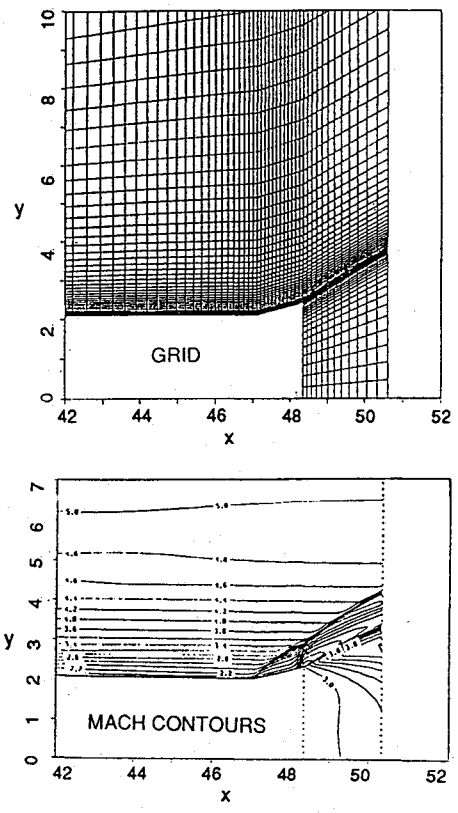

Fig. 9 Pegasus plume interference predictions, $M_\infty = 5$.

nose. These results are used as starting conditions for a parabolized Navier-Stokes (PNS) calculation using the UPS code[23] from NASA Ames Research Center. The PNS calculation produces a nonseparated viscous solution in a very efficient manner, since it uses a marching-type solution procedure. Turbulence in the fuselage boundary layer is modeled using the Baldwin-Lomax algebraic turbulence model.[24]

The grid used for the PNS calculations, 100 × 82 points in the streamwise and body-normal directions, respectively, was sufficient to insure adequate resolution of the fuselage boundary layer. At the upstream boundary, flow conditions obtained from the blunt-body calculation were imposed, and freestream conditions were applied at the far-field boundary, which is located just beyond the nose bow shock. Each PNS calculation required approximately 15 min on the NAS Cray-2.

Axisymmetric Navier-Stokes Solutions

The results of the PNS calculation were used as initial conditions for a Navier-Stokes calculation in the region of the first-stage rocket nozzle. These calculations were performed using the axisymmetric Navier-Stokes solver in the TURF code[25] from NASA Ames Research Center. Turbulence is modeled with the k-ε equations.

The grid used for the Navier-Stokes analysis of the base flow has 78 × 100 points in the streamwise and normal directions, respectively. The PNS results were applied at the upstream boundary, and the far-field boundary was treated as described above. A conical inviscid flow corresponding to the design rocket nozzle conditions was applied at the nozzle exit plane. These Navier-Stokes computations required approximately 15 min on the NAS Cray-2.

Predicted Mach number contours at $M_\infty = 5$ are shown in Fig. 9. An oblique shock occurs due to the presence of the ramp at the rocket nozzle, and at higher Mach numbers (and altitudes), the spreading of the plume induces a second oblique shock, which intersects the first shock, creating a lambda shock near the ramp. The pressure jump across the oblique shocks increases with Mach number. In all cases, the flow remains attached, even for the highest Mach number, where the plume expansion is largest. These results are strictly valid only for the higher-Mach-number cases in the flight profile, where the angle of attack is small; however, since the plume expands less at lower Mach numbers and altitude, it is unlikely that plume-induced flow separation is a critical problem.

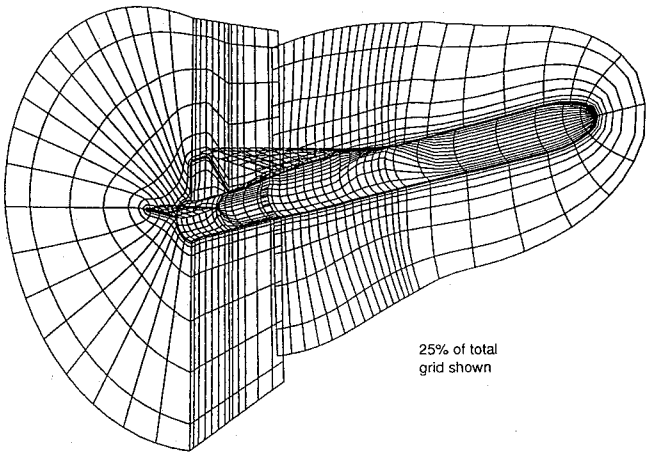

Fig. 10 Pegasus grid for three-dimensional Navier-Stokes calculations, $M_\infty = 5$.

As an interesting side benefit, surface heat transfer rates derived from the CFD calculations provided a check on thermal calculations made for the design of Pegasus's thermal protection system. The predicted boundary-layer thickness provided verification that adverse effects on control-fin loading on the portion of the fins submerged in the boundary layer were not a problem. The boundary-layer and Mach-number profiles near the body also helped identify a possible heating problem on the control-fin actuators.

Three-Dimensional Navier-Stokes Solutions

In early analyses of Pegasus, there was concern over possible deleterious effects from interaction between the shock waves produced by the wing and tail leading edges and the boundary layer on the body. The concern involved flow separation due to the shock-wave boundary-layer interaction and increased heat transfer due to the high compression of the flow through the shock coming in contact with the body surface. Each of these conditions could affect the design of the thermal protection system. A two-phase CFD analysis, using a complete three-dimensional model of Pegasus, examined the possibility of these adverse effects. The first phase involved a model of the fuselage and wing for two distinct flow conditions: 1) $M_\infty = 1.2$, $\alpha = 20$ deg, and 2) $M_\infty = 5$, $\alpha = 5$ deg. The second phase addressed the modeling of the complete Pegasus configuration for calculations at the higher Mach number.

Development of the computational grid is a major part of any CFD study, and Pegasus is no exception. The Chimera composite-grid approach[26] was chosen for the discretization process to achieve an accurate model of the entire configuration. The grid required for simulating the flow field around Pegasus was composed of two sections. The first section enclosed the body and wing, extending one grid cell beyond the trailing edge of the wing. The second section extended from the wing trailing edge to the base of the body. For the forward section, because of the blunt nose and the thick, round-edged wing, the grid was generated using the NASA Ames Research Center code HYGRIIID,[27] a three-dimensional hyperbolic grid generator. For the aft section, because of the simpler, more cylindrical geometry, the grid was generated using a NEAR code, HYPDAPT,[28] a two-dimensional hyperbolic grid generator. The two-dimensional grid generator was applied to compute grids in cross sections, which were combined to create a fully three-dimensional grid.

The final grid is presented in Fig. 10, where part of the grid on the surface of the body and wings is shown, along with the grid in the cross section at the trailing edge of the tail fins and in the plane of symmetry. Only 25% of the actual grid points are shown for clarity. The final cross section of the forward section is normal to the body in order to match more easily with the cross sections of the grid on the aft section. Note that a plane of symmetry was used to save computer time for longitudinal calculations. The forward grid contains 92 × 83 × 51 points, and the aft grid contains 54 × 83 × 51 points, a total of 618,018 points.

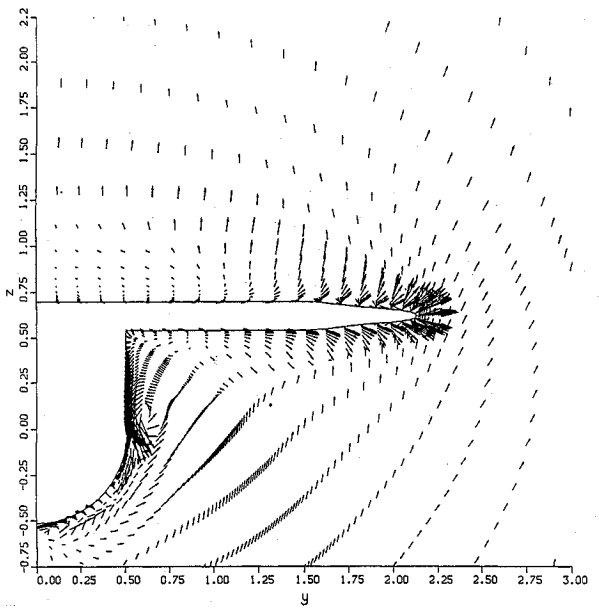

a) Flow vectors

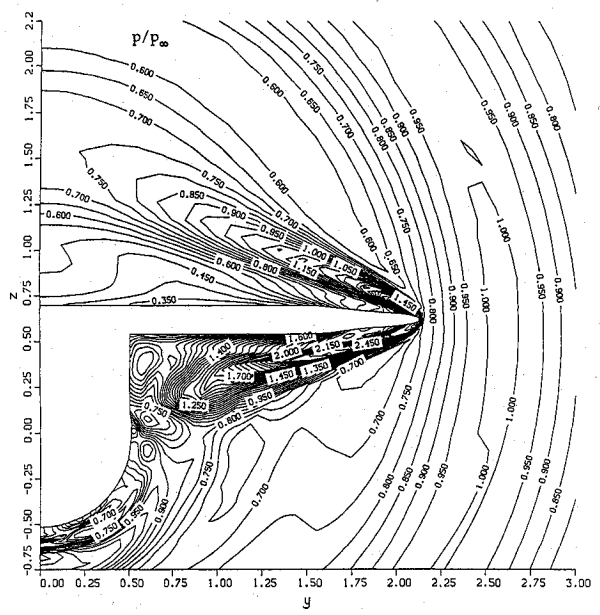

b) Pressure contours

Fig. 11 Predicted flow characteristics in the vicinity of the Pegasus wing fillet, $M_\infty = 5, \alpha = 5$ deg.

The computation of the flowfield was carried out using the F3D code[29] from NASA Ames Research Center. The code solves the compressible three-dimensional thin-layer Navier-Stokes equations, uses upwind spatial differencing in a streamwise direction, and is either first-order or second-order accurate in space. For the calculations described herein, the accuracy in time is first order.

Numerical computations on the complete Pegasus configuration were carried out at $M_\infty = 5$ and $\alpha = 5$ deg for a Reynolds number of 1.33×10^6. A total of about 25 h of CPU time on the Cray-2 computer was required for these calculations.

A typical outcome of a CFD computation is a large quantity of information that is difficult to assimilate using traditional methods. For example, results include surface streamlines, flowfield velocity vectors, and surface pressure contours on the entire configuration; therefore, careful examination can reveal many interesting details about the flow around the vehicle. Flowfield vectors and pressure contours are shown in Fig. 11 at a station aft of the wing root chord leading edge to illustrate the flow in the region of the wing-fuselage fairing. These details show a separated region beneath the wing and the approximate position of the wing leading edge shock wave. It was an initial concern that the wing shock wave could impinge on the fuselage and fairing and cause heating problems. It appears from the computations that the wing shock wave never reaches the fuselage surface. Further examination of results aft of this station show vortices on top of the fairing behind the wing, and, in the tail region, the vortex from the fairing seems to get "trapped" at the base of the rudder.

Conclusions

A major conclusion is an evaluation of the design capabilities of a number of the codes currently available to the missile design community. Though only a few of the available codes were used in this study, the experience illustrates the requirements for useful prediction methods at all levels of complexity.

In the preliminary design application, a number of codes are available that can provide moderately accurate results at a reasonable cost. They are generally available and easy to use, and for moderate flight conditions there is good agreement in the results from different methods. For extreme flight conditions at high angles of attack, codes that include effects of nonlinearities are required; for example, Missile DATCOM and MISL3 are complementary methods, each providing a necessary portion of the aerodynamic characteristics.

As the level of complexity increases and as more detailed information is needed, engineering-level codes, generally in the form of panel methods, are available. It is essential that codes on this level also include nonlinear effects associated with body vortices and lifting-surface leading-edge vorticity. The cost of these codes in both engineering time and computation time increases with the level of information produced, but the need for aerodynamic load distributions and vortex-induced effects makes the extra effort justified. The use of these codes to check results from the preliminary design codes at selected flow conditions proved to be a valuable technique to increase confidence in the results from the simpler codes.

Finally, the use of CFD codes for practical application to design problems is becoming more feasible as the codes are further developed. Their use will only continue to increase as the codes become better and easier to use and computers run faster.

The use of Navier-Stokes codes for missile design is still in the preliminary or research stage. Their use is restricted to very special problems that cannot be solved in any other manner; for example, flow problems involving flow separation or other viscous phenomena. These codes are not yet available to many small missile-design groups because of the difficulty using them and the high cost involved with solutions. In spite of the current disadvantages, CFD will soon be a readily available analysis tool for missile designers.

Epilogue

Initial test flights on the B-52 were made in early 1990 to check out the Pegasus systems and carriage loads. It was verified that actual carriage loads imposed on the B-52 pylon were well within the predicted levels. On April 5, 1990, the first drop and flight of Pegasus was accomplished successfully. The second flight occurred on July 17, 1991. In both flights, Pegasus cleared the B-52 safely as predicted, the aerodynamic portion of the mission profile was completed as planned, and, most importantly, payloads were placed into orbit. Comparison of measured and predicted aerodynamic characteristics of Pegasus will be the subject of a future paper.

Acknowledgments

Parts of the CFD effort and the preparation of this article were funded by a NEAR IR&D program. The authors thank the Orbital Sciences Corporation for the sponsorship of the technical investigation reported herein. The personnel and facilities of the Numerical

Aerodynamic Simulator (NAS) at the NASA Ames Research Center are thanked for their assistance and advice in the use of a number of research CFD codes for the analysis of Pegasus.

References

[1]Mendenhall, M. R., Lesieutre, D. J., Caruso, S. C., Dillenius, M. F. E., and Kuhn, G. D., "Aerodynamic Design of Pegasus—Concept to Flight with CFD," presented at AGARD Symposium on Missile Aerodynamics, Friedrichshafen, Germany, April 1990.

[2]Baker, W. B., Jr., "Use of Semiempirical Aerodynamic Methods for Preliminary Design," *Missile Aerodynamics; Proceedings*, Nielsen Engineering & Research, Nov. 1989.

[3]Lesieutre, D. J., Mendenhall, M. R., Nazario, S. M., and Hemsch, M. J., "Prediction of the Aerodynamic Characteristics of Cruciform Missiles Including Effects of Roll Angles and Control Deflections," NEAR TR 360, Nielsen Engineering & Research, Mountain View, CA, Aug. 1986.

[4]Lesieutre, D. J., Dillenius, M. F. E., Mendenhall, M. R., and Torres, T. O., "Aerodynamic Analysis Program MISL3 for Conventional Missiles with Cruciform Fin Sections," NEAR TR 404, Nielsen Engineering & Research, Mountain View, CA, Dec. 1989.

[5]Vukelich, S. R., Stoy, S. L., Burns, K. A., Castillo, J. A., and Moore, M. E., "MISSILE DATCOM, Volume I— Final Report," AFWAL-TR-86-3091, Wright-Patterson AFB, OH, Dec. 1988.

[6]Vukelich, S. R., and Jenkins, J. E., "Missile Datcom: Aerodynamic Prediction of Conventional Missiles Using Component Build-Up Techniques," AIAA Paper 84-0388, Jan. 1984.

[7]Gentry, A. E., Smyth, D. N., and Oliver, W. R., "The Mark IV Supersonic-Hypersonic Arbitrary-Body Program," AFFDL TR-73-159, Wright-Patterson AFB, OH, Nov. 1973.

[8]Williams, J. E., Matthews, B. L., Adiasor, M. I., and Casey, L. E., "Missile Aerodynamic Design Method (MADM)," AFWAL-TR-87-3109, Wright-Patterson AFB, OH, Feb. 1988.

[9]Lesieutre, D. J., Mendenhall, M. R., Nazario, S. M., and Hemsch, M. J., "Aerodynamic Characteristics of Cruciform Missiles at High Angles of Attack," AIAA Paper 87-0212, Jan. 1987.

[10]Lesieutre, D. J., Mendenhall, M. R., and Dillenius, M. F. E., "Prediction of Induced Roll on Conventional Missiles with Cruciform Fin Sections," AIAA Paper 88-0529, Jan. 1988.

[11]Stoy, S. L., and Vukelich, S. R., "Prediction of Aerodynamic Characteristics of Unconventional Missile Configurations Using Component Build-up Techniques," AIAA Paper 86-0489, Jan. 1986.

[12]Covell, P. F., "Supersonic Aerodynamic Characteristics of Canard, Tailless, and Aft-Tail Configurations for Two Wing Planforms," NASA TP 2434, June 1985.

[13]Dillenius, M. F. E., Perkins, S. C., Jr., and Lesieutre, D. J., "Modified NWCDM-NSTRN and Supersonic Store Separation Programs for Calculating NASTRAN Forces Acting on Missiles Attached to Supersonic Aircraft," NWC TP 6834, China Lake, CA, Sept. 1987.

[14]Lesieutre, D. J., Dillenius, M. F. E., and Whittaker, C. H., "Program SUBSAL and Modified Subsonic Store Separation for Calculating NASTRAN Forces Acting on Missiles Attached to Subsonic Aircraft," NEAR TR 393, Nielsen Engineering & Research, Mountain View, CA, Dec. 1991.

[15]Dillenius, M. F. E., Goodwin, F. K., and Nielsen, J. N., "Extension of the Method for Predicting Six-Degree-of-Freedom Store Separation Trajectories at Speeds up to the Critical Speed to Include a Fuselage with Noncircular Cross Section, Vol. I—Theoretical Methods and Comparisons with Experiment," AFFDL-TR-74-130, Wright-Patterson AFB, OH, Nov. 1974.

[16]Goodwin, F. K., and Smith, C. A., "Theoretical Separation Characteristics of Two Conceptual Solid Rocket Booster Parachute Test Units From the B-52 Aircraft," NEAR TR 114, Nielsen Engineering & Research, Mountain View, CA, Aug. 1976.

[17]Dillenius, M. F. E., Goodwin, F. K., and Nielsen, J. N., "Analytical Prediction of Store Separation Characteristics from Subsonic Aircraft," *Journal of Aircraft*, Vol. 12, Oct. 1975, pp. 812–818.

[18]Matranga, G. J., "Launch Characteristics of the X-15 Research Airplane as Determined in Flight," NASA TN D-723, Feb. 1961.

[19]Walker, H. J., and Wolowicz, C. H., "Theoretical Stability Derivatives for the X-15 Research Airplane at Supersonic and Hypersonic Speeds Including a Comparison with Wind-Tunnel Results," NASA TM X-287, Aug. 1960.

[20]Yancy, R. B., "Flight Measurements of Stability and Control Derivatives of the X-15 Research Airplane to a Mach Number of 6.02 and an Angle of Attack of 25°," NASA TN D-2532, Nov. 1964.

[21]Priolo, F. J., and Wardlaw, A. B., Jr., "A Comparison of Inviscid Computational Methods for Supersonic Tactical Missiles," AIAA Paper 87-0113, Jan. 1987.

[22]Hsieh, T., and Priolo, F. J., "Generation of the Starting Plane Flowfield for Supersonic Flow over a Spherically Capped Body," NSWC TR 84-484, Naval Surface Weapons Center, Dahlgren, VA, May 1985.

[23]Lawrence, S. L., Tannehill, J. C., and Chauseee, D. S., "An Upwind Algorithm for the Parabolized Navier-Stokes Equations," AIAA Paper 86-1117, May 1986.

[24]Baldwin, B. S., and Lomax, H., "Thin Layer Approximation and Algebraic Model for Separated Turbulent Flows," AIAA Paper 78-0257, Jan. 1978.

[25]Coakley, T. J., "Implicit Upwind Methods for the Compressible Navier-Stokes Equations," *AIAA Journal*, Vol. 23, March 1985, pp. 374–380.

[26]Buning, P. G., Chiu, I.T., Obayashi, S., Rizk, Y. M., and Steger, J. L., "Numerical Simulation of the Integrated Space Shuttle Vehicle in Ascent," AIAA Paper 88-4359, Aug. 1988.

[27]Rizk, Y. M., Steger, J. L., and Chaussee, D., "Use of a Hyperbolic Grid Generation Scheme in Simulating Supersonic Viscous Flow about Three-Dimensional Winged Configurations," NASA TM 86776, July 1985.

[28]Klopfer, G. H., "Solution Adaptive Meshes with a Hyperbolic Grid Generator," *2nd International Conference on Numerical Grid Generation in Computational Fluid Dynamics*, Pineridge Press, Mumbles, Swansea, Wales, UK, Dec. 1988, pp. 443–454.

[29]Ying, S. X., Steger, J. L., and Schiff, L. B., "Numerical Simulation of Unsteady, Viscous, High Angle-of-Attack Flows Using a Partially Flux-Split Algorithm," AIAA Paper 86-2179, Aug. 1986.